Journal of Mass Spectrometry and Advances in the Clinical Lab 25 (2022) 27–35

Contents lists available at ScienceDirect

Journal of Mass Spectrometry and Advances in the Clinical Lab

journal homepage: www.sciencedirect.com/journal/journal-of-mass-spectrometry-and-advances-in-the-clinical-lab

Development and validation of a paper spray mass spectrometry method for the rapid quantitation of remdesivir and its active metabolite, GS-441524, in human plasma

Christine Skaggs [a], Hannah Zimmerman [a], Nicholas Manicke [a,b], Lindsey Kirkpatrick [c,*]

[a] Department of Chemistry and Chemical Biology, Indiana University-Purdue University Indianapolis, Indianapolis, IN 46202, USA
[b] Forensics and Investigative Sciences, Indiana University-Purdue University Indianapolis, Indianapolis, IN 46202, USA
[c] Department of Pediatrics, Division of Pediatric Infectious Diseases, Indiana University School of Medicine, Indianapolis, IN 46202, USA

ARTICLE INFO

Keywords:
SARS-CoV-2
Remdesivir
Antiviral
Paper spray
Mass spectrometry

ABSTRACT

Introduction: Remdesivir (GS-5734) is a nucleoside analog prodrug with antiviral activity against several single-stranded RNA viruses, including the novel severe respiratory distress syndrome virus 2 (SARS-CoV-2). It is currently the only FDA-approved antiviral agent for the treatment of individuals with COVID-19 caused by SARS-CoV-2. However, remdesivir pharmacokinetics/pharmacodynamics (PK/PD) and toxicity data in humans are extremely limited. It is imperative that precise analytical methods for the quantification of remdesivir and its active metabolite, GS-441524, are developed for use in further studies. We report, herein, the first validated antiviral paper spray-mass spectrometry (PS-MS/MS) assay for the quantification of remdesivir and GS-441524 in human plasma. We seek to highlight the utility of PS-MS/MS technology and automation advancements for its potential future use in clinical research and the clinical laboratory setting.

Methods: Calibration curves for remdesivir and GS-441524 were created utilizing seven plasma-based calibrants of varying concentrations and two isotopic internal standards of set concentrations. Four plasma-based quality controls were prepared in a similar fashion to the calibrants and utilized for validation. No sample preparation was needed. Briefly, plasma samples were spotted on a paper substrate contained within pre-manufactured plastic cassette plates, and the spots were dried for 1 h. The samples were then analyzed directly for 1.2 min utilizing PS-MS/MS. All experiments were performed on a Thermo Scientific Altis triple quadrupole mass spectrometer utilizing automated technology.

Results: The calibration ranges were 20 – 5000 and 100 – 25000 ng/mL for remdesivir and GS-441524, respectively. The calibration curves for the two antiviral agents showed excellent linearity (average R^2 = 0.99–1.00). The inter- and intra-day precision (%CV) across validation runs at four QC levels for both analytes was less than 11.2% and accuracy (%bias) was within ± 15%. Plasma calibrant stability was assessed and degradation for the 4 °C and room temperature samples were seen beginning at Day 7. The plasma calibrants were stable at −20 °C. No interference, matrix effects, or carryover was discovered during the validation process.

Conclusions: PS-MS/MS represents a useful methodology for rapidly quantifying remdesivir and GS-441524, which may be useful for clinical PK/PD, therapeutic drug monitoring (TDM), and toxicity assessment, particularly during the current COVID-19 pandemic and future viral outbreaks.

Abbreviations: ANOVA, A one-way analysis of variance; AUC, area under the curve; CE, collision energy; CES1, carboxylesterase-1; CES2, carboxylesterase-2; R^2, coefficient of determination; CV, coefficient of variation; DMSO, dimethyl sulfoxide; EC50, half maximum effective concentration; ECMO, extracorporal membrane oxygenation; H-ESI, heated electrospray ionization; Inc, Incorporated; IRB, institutional review board; IS, internal standard; kV, kilovolts; LC-MS/MS, liquid chromatography–mass spectrometry; LLC, Limited Liability Company; LOD, limit of detection; LLOQ, lower limit of quantitation; *m/z*, mass-to-charge; µg, microgram; µL, microliter; mL, milliliter; MP, monophosphate; ng, nanogram; PS-MS/MS, paper spray–mass spectrometry; PK, pharmacokinetics; PD, pharmacodynamics; RF, radio frequency; S/B, Signal-to-Blank; SS, spiking solution; SIL, stable isotopically-labeled; therapeutic drug monitoring, TDM; QC, quality control; QC-LLOQ, quality control-lower limit of quantification; V, volts.

* Corresponding author.
E-mail address: lkirkpat@iupui.edu (L. Kirkpatrick).

https://doi.org/10.1016/j.jmsacl.2022.06.001
Received 2 November 2021; Received in revised form 21 May 2022; Accepted 1 June 2022
Available online 11 June 2022
2667-145X/© 2022 THE AUTHORS. Publishing services by ELSEVIER B.V. on behalf of MSACL. This is an open access article under the CC BY-NC-ND license (http://creativecommons.org/licenses/by-nc-nd/4.0/).

1. Introduction

The emergence of severe acute respiratory coronavirus 2 (SARS-CoV-2) in 2019 resulted in an ongoing world-wide pandemic with more than 4.5 million deaths reported as of October 2021 according to the World Health Organization (WHO), and this number is thought to be drastically underestimated [1–3]. Remdesivir, also known as GS-5734 (Gilead Sciences, Inc, Foster City, CA), is the first and only FDA-approved antiviral drug that has been used as a possible treatment for SARS-CoV-2, which causes COVID-19. Prior to the SARS-CoV-2 pandemic, remdesivir had been researched as a treatment for single-stranded RNA viruses, including several other coronaviruses and ebolavirus [4]. Briefly, remdesivir is a prodrug of an adenosine nucleotide analogue [5,6]. Remdesivir is metabolized within cells to its alanine metabolite (GS-704277) followed by formation of GS-441524. GS-441524 then undergoes rapid phosphorylation into the monophosphate derivative (GS-441524-MP) followed by formation of the active nucleoside triphosphate derivative (GS-443902) [6]. The active derivative binds to the viral RNA-dependent RNA polymerase, which terminates RNA transcription, thereby inhibiting viral replication [6]. GS-441524, the nucleoside core of remdesivir, also has some antiviral activity and has been found to diffuse into cells. In fact, an animal study conducted in Rhesus monkeys showed that remdesivir was rapidly eliminated with a short plasma half-life of ~0.4 h with transient emergence of the alanine intermediate metabolite intracellularly followed by the appearance of GS-441524 [7]. In addition, the nucleoside triphosphate derivative forms rapidly and achieves a maximum intracellular concentration in four hours (half-life = ~16 ± 1 h) [7].

Remdesivir has been shown to be beneficial in the treatment of COVID-19 in a few clinical trials to date. A cohort of 53 patients with severe symptoms from SARS-CoV-2 infection, receiving remdesivir through compassionate use, showed clinical improvement with its use; however, 60% reported adverse events at follow-up [8]. The most common adverse events reported were increased hepatic enzymes (23%), diarrhea (9%), rash (8%), renal impairment (8%), and hypotension (8%). In a multicenter, double-blind, randomized, placebo-controlled clinical trial to evaluate the safety and efficacy of remdesivir in hospitalized adults diagnosed with COVID-19 with evidence of lower respiratory tract infection, remdesivir was shown to be superior to placebo in shortening the time to recovery [9]. 131 of 532 patients in the remdesivir arm (24.6%) were reported to have serious adverse events while receiving remdesivir. Other clinical trials have been inconclusive as far as efficacy, but these studies have several limitations [10,11]. Overall, remdesivir efficacy in its treatment of COVID-19 remains a topic of debate. At present, there are several ongoing clinical trials to study its efficacy and safety in broader patient populations.

Although remdesivir is an FDA-approved medication for COVID-19, little is known about its pharmacokinetics and pharmacodynamics (PK/PD) in humans. The initial PK/PD studies in early phase clinical trials were conducted in Rhesus monkeys and healthy adults to help determine dosing and assess safety. In these studies, both remdesivir and GS-441524 exhibited linear pharmacokinetics following single doses between 3 mg and 225 mg [12]. In multiple-dose studies of remdesivir (150 mg once daily for 7 or 14 days), the PK profile was similar to single-dose administration [12]. There were few reported adverse events in these healthy human cohorts. There are no PK/PD data available for individuals infected with COVID-19, nor are there any data available for other special patient populations, such as children, women who are pregnant or breast feeding, individuals who are critically-ill, individuals with renal or hepatic impairment, or individuals requiring dialysis or extracorporeal membrane oxygenation (ECMO) [13]. As the dosage of remdesivir for use in COVID-19 was largely derived from *in vitro* half maximum effective concentration (EC50) experiments for SARS-CoV-2 and the initial pharmacokinetic studies utilizing healthy adults, the current dosage regimens may not translate well in COVID-19 patients and special patient populations due to alterations in pharmacokinetics [12]. With the lack of PK/PD data in these patients, it is possible that current dosage regimens may lead to sub-therapeutic concentrations, which could explain variable study outcomes [8–11]. Another significant concern is toxicity, as severe adverse events have been frequently reported with remdesivir [8–11,14]. In particular, drug-drug interactions, nephrotoxicity, and hepatic toxicity are important safety concerns. Remdesivir is an ester prodrug, and hydrolysis is required for its therapeutic activity. It has been confirmed that remdesivir is hydrolytically-activated by carboxylesterase-1 (CES1) [15]. However, excessive hydrolysis has been shown to result in severe cytotoxicity by inhibiting proliferation and enhancing apoptosis, particularly in liver tissue. In addition, the use of glucocorticoids (commonly-utilized in individuals with COVID-19) can induce CES1 and further increase cytotoxic effects [16]. Remdesivir has also been shown to irreversibly inhibit carboxylesterase-2 (CES2), a major hydrolase, which may further contribute to other drug-drug interactions [17]. Thus, there is a need to generate more PK/PD data to optimize dosage strategies, and TDM may be required to individualize dosing regimens to improve overall efficacy and safety.

Despite the urgent need, few precise analytical methods for the quantification of remdesivir and GS-441524 have been described in the literature [18–23]. The few methods reported have all utilized LC-MS/MS with protein precipitation sample preparations of varying difficulty and run times ranging from 3 to 10 min. Overall, mass spectrometry-based approaches are attractive due to their high sensitivity, high specificity, lack of interference, multiplexing capability, low reagent cost, and high throughput [24]. However, the need for specific technical expertise, lack of automation, and tedious sample preparation often hinder implementation within institutional clinical laboratories, and, hence, patient samples must be shipped to reference laboratories, which can negatively impact patient care due to lengthy turn-around times [24,25]. New methods are needed that eliminate some of these barriers in order to be implemented near the point-of-care.

Paper spray (PS), an ambient ionization technique, is an ideal method for qualitative and quantitative analysis, as it allows for the direct analysis of complex biological samples [26–28]. Briefly, a small sample volume (<10 uL) is spotted onto a pointed paper substrate and allowed to dry for 1 h. Analyte ions are generated directly from the dried spot via application of a spray solvent (30–200 μL) and a high voltage (3 kV–5 kV) while the sharp tip of the paper is in close proximity to the inlet of an unmodified mass spectrometer. The gas-phase ions then enter the mass spectrometer for analysis [29]. Paper spray-mass spectrometry (PS-MS/MS) assays have been developed for clinical drug measurements including immunosuppressives [30,31], anti-microbials [32,33], cancer drugs [34,35], and others [36–39]. PS-MS/MS has several advantages when compared to liquid chromatography – mass spectrometry (LC-MS/MS) methods, including no sample preparation, elimination of chromatography instrumentation, lower solvent consumption, lower sample volumes, and faster turnaround times [28–31,39,40]. Overall, there is less need for significant expertise to operate and troubleshoot the instrumentation, and the lack of sample preparation is beneficial to the clinical laboratory workflow. In addition, there have been strides made in the development of automated PS systems and plug-and-play software for ease of use. Herein, we present the first validated PS- MS/MS method for the simultaneous quantitation of remdesivir and its active nucleoside core, GS-441524, in plasma samples. Experiments were carried out on an automated system utilizing the Thermo Scientific Verispray paper spray source with plate-loading magazine unit and Altis triple quadruple mass spectrometer. This method provides a suitable alternative to the few reported LC-MS/MS methods for TDM and multiple-dose pharmacokinetic studies.

2. Materials and methods

2.1. Chemicals and reagents

Analytical-grade acetonitrile, dimethyl sulfoxide (DMSO), methanol, and water were purchased from Fisher Scientific (Pittsburgh, PA, USA). Formic acid was purchased from Sigma Aldrich (St. Louis, MO, USA). Remdesivir and GS-441524 were purchased from Cayman Chemical, Inc (Ann Arbor, MI, USA). GS-441524-13C5 was purchased from Cambridge Isotope Laboratories, Inc (Tewksbury, MA, USA) Remdesivir-D5 and GS-704277 were purchased from MedChemExpress, LLC (Monmouth Junction, NJ, USA). Captisol was purchased from VWR International, LLC (Radnor, PA, USA).

2.2. Sample preparation

Individual 1 mg/mL stock solutions of remdesivir and GS-441524 were prepared in DMSO. Seven spiking solutions were prepared (SS1 – 7) in methanol. The concentrations were as follows: 100 μg/mL (SS1), 50 μg/mL (SS2), 10 μg/mL (SS3), 4 μg/mL (SS4) 2 μg/mL (SS5), 1 μg/mL (SS6), 200 ng/mL (SS7) for remdesivir and 500 μg/mL (SS1), 250 μg/mL (SS2), 50 μg/mL (SS3), 20 μg/mL (SS4) 10 μg/mL (SS5), 5 μg/mL (SS6), 2 μg/mL (SS7) for GS-441524. Stock and spiking solutions were stored at −20 °C until use. Plasma calibrants were prepared by spiking a 95 μL aliquot of plasma with 5 μL of the corresponding spiking solution (SS1–SS7) to make final plasma concentrations of 5000 ng/mL, 2500 ng/mL, 500 ng/mL, 200 ng/mL, 100 ng/mL, 50 ng/mL, 20 ng/mL and 25000 ng/mL, 12500 ng/mL, 2500 ng/mL, 1000 ng/mL, 500 ng/mL, 250 ng/mL, 100 ng/mL for remdesivir and GS-441524, respectively. Remdesivir-D5 and GS-441524-13C5 were dissolved in DMSO to make stock solutions of 5 mg/mL and 1 mg/mL, respectively. An internal standard spiking solution was prepared in methanol with final concentrations of 40 μg/mL for remdesivir-D5 and 200 μg/mL for GS-441524-13C5. Then, 5 μL of the internal standard (IS) spiking solution was spiked into each plasma calibrant with final IS concentrations of 200 ng/mL for remdesivir-D5 and 1000 ng/mL for GS-441524-13C5. After preparation, samples were spotted onto the paper substrate (8 μL) and allowed to dry under ambient conditions for 1 h.

Internal quality controls (QCs) were prepped similarly to the plasma calibrants. Spiking solutions were prepared as follows: 100 μg/mL (QCSS1), 10 μg/mL (QCSS2), 5 μg/mL (QCSS3), 1.6 μg/mL (QCSS4) and 500 μg/mL (QCSS1), 50 μg/mL (QCSS2), 25 μg/mL (QCSS3), 8 μg/mL (QCSS4) for remdesivir and GS-441524, respectively. QCs were stored under the same conditions as their plasma calibrant counterparts. The QCs were prepared by spiking a 95 μL aliquot of plasma with 5 μL of the corresponding spiking solution (QCSS1 – QCSS4) to make final plasma concentrations of 5000 ng/mL, 500 ng/mL, 250 ng/mL, 80 ng/mL and 25000 ng/mL, 2500 ng/mL, 1250 ng/mL, 400 ng/mL for remdesivir and GS-441524, respectively. Then, 5 μL of the IS spiking solution were spiked into each plasma QC as was done with the plasma calibrants. The final IS concentrations in the plasma QCs were 200 ng/mL for remdesivir-D5 and 1000 ng/mL for GS-441524-13C5, respectively. Samples were spotted onto the paper substrate (8 μL) and allowed to dry for 1 h.

For the degradation studies, two separate sets of plasma QCs and plasma calibrants were prepared according to the procedures stated above. The first set of QCs were spotted onto the paper substrate of the pre-made plastic cassette plates, allowed to dry for 1 h, covered, and stored at three different temperatures, 22 °C, 4 °C, and −20 °C. The second set of QCs was aliquoted into three separate sets of vials, and stored under the three different temperature conditions. Samples were then run on days 0, 7, 14, and 21 to assess stability of the dried spot and plasma calibrants.

2.3. Paper spray mass spectrometry assay development

Mass spectrometric conditions were optimized using continuous infusion of remdesivir, remdesivir-D5, GS-441524, and GS-441524-13C5 into a Thermo Scientific heated electrospray ionization (H-ESI) source by a syringe pump. Selected reaction monitoring (SRM) transitions for all analytes were selected accordingly and are listed in Table 1. All conditions and SRMs were confirmed via PS-MS/MS prior to moving forward with validation.

Paper spray (PS) was performed utilizing pre-made plastic cassette plates containing Whatman grade 31ET chromatography paper purchased from Thermo Fisher Scientific (Product number: VSSP1-10000; San Jose, CA, USA). An automated PS source, Verispray (San Jose, CA, USA), with a plate-loading magazine unit was coupled to a Thermo Fisher Scientific TSQ Altis triple quadrupole mass spectrometer (San Jose, CA, USA). A solvent mixture of 90%:10% acetonitrile:water with 0.1% formic acid was utilized as the spray solvent. Formic acid was included to aid in ionization through protonation. Optimized mass spectrometry parameters were as follows: 270 °C capillary temperature, 4300 V spray voltage, positive ion mode, and no sheath or auxiliary gas.

Table 1
The analytes and stable isotopic internal standards investigated, molecular formulas, parent ions (*m/z*), fragment ions (*m/z*), RF lens values, and collision energy (CE) parameters. The quantifier fragment ion is shown in bold.

Compound	Formula	Parent Ion (*m/z*)	Fragment ions (*m/z*)	Collision Energy (V)	RF Lens (V)
Remdesivir	$C_{27}H_{35}N_6O_8P$	603	**200**	38	91
			229	21	
			318	20	
			402	16	
Remdesivir-D5	$C_{27}H_{30}D_5N_6O_8P$	608	**205**	38	74
			229	27	
			407	14	
			323	21	
GS-441524	$C_{12}H_{13}N_5O_4$	292	**202**	13	103
			147	31	
			163	26	
			173	26	
GS-441524-13C5	$C_7[^{13}C_5]H_{13}N_5O_4$	297	**204**	13	74
			148	31	
			164	26	
			174	26	

The instrument was operated in SRM mode with a dwell time of 98 ms. The automated Verispray source parameters were sample rewetting A: 1 (10 μL), spray solvent B: 15 (150 μL). Sample run time was 1.2 min.

2.4. Method validation

Validation procedures utilized FDA guidelines for bioanalytical method validation as a framework where each analytical run consisted of plasma calibrants, internal QCs, blanks with internal standard, and double blanks without internal standard [41]. Calibration curves were run in duplicate, one at the beginning and one at the end of each experimental run. Assay linearity was assessed utilizing seven plasma-based calibrants. The calculated limit of detection (LOD) was defined as three times the standard error of the intercept divided by the slope (3* (standard error of the intercept/slope)). The calculated lower limit of quantitation (LLOQ) was defined as ten times the standard error of the intercept divided by the slope (10*(standard error of the intercept/slope)). The measured LLOQ is representative of the QCs with the lowest concentration. Two or more replicates of each QC were performed per analytical run. More than 67% of all QCs and 50% of QCs at each concentration level had to meet the acceptance criterion of a difference of ≤ 25% of the known nominal concentration for the analytical run to be considered valid. Plasma blanks with internal standard and plasma double blanks were used to assess the carryover and blank signal. Relative matrix effects were assessed using a method developed by Matuszewski, *et al.*, by preparing calibration curves in multiple six donor lots of plasma and assessing the overall variation of the calibration slopes across the donor lots [42].

2.5. Assessment of Endogenous, exogenous and metabolic interferences

Hemolysis was assessed in accordance with established protocols [43]. Briefly, fresh drug-free whole blood was shaken vigorously and stored at −20 °C for 30 min. Hemolyzed blood was spiked into blank plasma to create two test groups consisting of 0.5% and 2% hemolyzed plasma. High and low concentration QCs utilizing plasma from the two test groups were prepared, and three replicates were run in duplicate and analyzed as described earlier. To be considered negligible, the

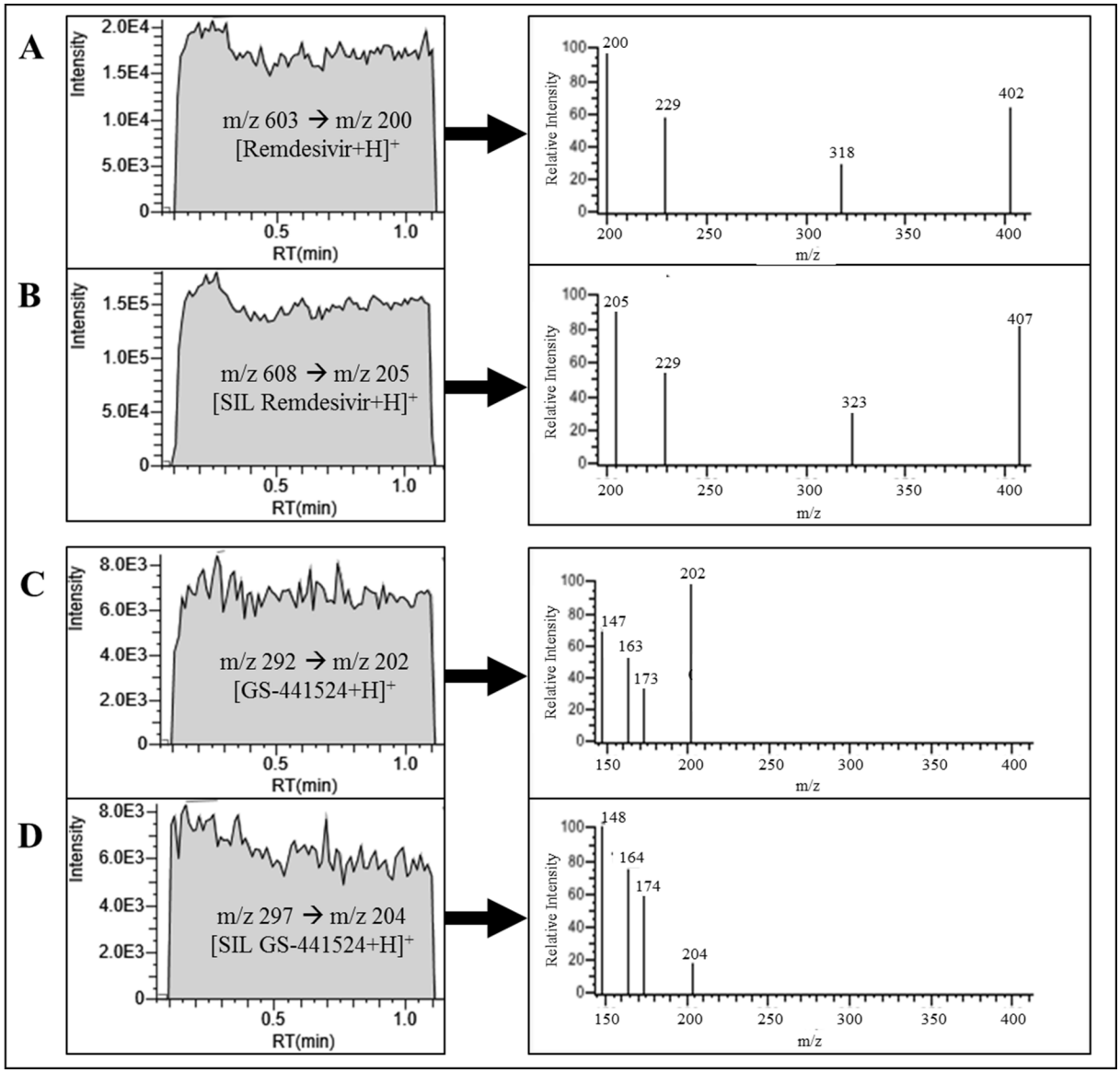

Fig. 1. Representative PS-MS/MS chronograms and spectra data for remdesivir and GS-441524. Left column shows the extracted ion chronograms for the [H +] adducts of remdesivir (A), SIL remdesivir internal standard (B), GS-441524 (C), and SIL GS-441524 internal standard (D). Right column shows the stick SRM spectra for the quantifier and confirmatory fragment ions to show expected ion ratios.

difference in nominal concentration between hemolyzed and non-hemolyzed samples had to be ≤ 25% for all analytes. Drug-free icteric and lipidemic plasma samples were collected from the Indiana University Health Pathology Laboratory and stored at −20 °C until use. QCs at the high and low levels were prepared in three separate lipidemic samples and three separate icteric samples and run in duplicate. QCs prepared in normal plasma were used as the control. To be considered negligible, lipidemic and icteric samples had to meet precision and accuracy acceptance criteria of ≤ 25% for all analytes.

To assess exogenous interference and metabolic interference, five replicates of a 1 μg/mL solution of Captisol, a cyclodextrin additive, or GS-704227, a known metabolite, was spiked into blank plasma. To assess interference from these molecules, an unequal variance two-sample *t*-test was run to compare the double blank to the spiked sample containing the interferent. Interference was not deemed statistically significant if the two-tailed *p*-value was greater than 0.05.

2.6. Identification and acceptance criteria

Identification can be confirmed when the ratio between the analyte quantifier and qualifier (confirmatory) SRM ions, averaged over the entire scan time, are within ± 25% of the expected value. For sample acceptance, the internal standard analyte area under the curve (AUC) should be within two standard deviations of the mean to pass. A batch is considered valid when the coefficient of determination (R^2) for the calibration curves is greater than 0.98, and more than 67% of all QCs and 50% of QCs at each concentration level meet the acceptance criterion of being ≤ 25% of the known nominal concentration.

2.7. Data acquisition and quantitation

The time required per sample analysis was 2.2 min, which included on-paper extraction (1 min) and the data collection period (1.2 min). SRM of the chosen quantifier ion was utilized for quantitation while the other transitions were used as qualifier, or confirmatory, ions. Chronograms and resulting SRM spectra showing the fragment quantifier and confirmatory ions are pictured in Fig. 1. Briefly, the AUC of the analyte quantifier fragment ion over the course of the analysis time was determined utilizing automatic peak integration. The AUC of the analyte quantifier fragment ion was divided by the AUC of the corresponding IS quantifier fragment ion to obtain the peak area ratio. The peak area ratios were then plotted against their known concentration to generate a calibration curve. No background subtraction was performed as it is substantially less than the analytical signal within the measurement range and has a negligible effect. A calibration curve was constructed by weighted linear regression from calibration standards analyzed within the same batch and used for calculation of all QCs for that batch.

2.8. Data processing and statistical analysis

Data analysis was performed utilizing Tracefinder v3.3 (Thermo Fisher Scientific Inc, San Jose, CA, USA). The calibration curves were calculated using 1/x weighted linear least squares [44]. All statistics were performed utilizing Minitab (Minitab Inc, State College, PA, USA) or Excel (Microsoft Corporation, Redmond, WA, USA).

2.9. Institutional review board approval

All lipidemic and icteric plasma samples utilized in the endogenous interference study were obtained from the Indiana University Health Pathology Laboratory. These remnant human samples were de-identified prior to use and handled in accordance with Institutional Review Board (IRB) protocol #2008090461.

Results

3.1. Method optimization

An extraction/spray solvent composition of 90% acetonitrile and 10% water with 0.1% formic acid was found to be optimal to generate signal with maximum intensity and stability for remdesivir and GS-441524. The four most intense product ions (1 quantifier ion and 3 qualifier (confirmatory) ions), corresponding collision energies, and radio frequency (RF) lens values were selected for each analyte during continuous syringe pump infusion electrospray ionization experiments (Table 1). The transitions for the quantifier ions were as follows: *m/z* 603 → 200 for remdesivir, *m/z* 608 → 205 for stable isotopically-labeled (SIL) remdesivir internal standard, *m/z* 292 → *m/z* 202 for GS-441524, and *m/z* 297 → 204 for the SIL GS-441524 internal standard. Optimal mass spectrometer instrument parameters were also determined during the electrospray ionization experiments. SRMs and instrument settings were confirmed utilizing PS-MS/MS prior to validation. An aliquot of 95uL of drug-free plasma for each calibrant was used, which is ideal in the event smaller sample volumes need to be obtained (e.g., pediatric individuals, anemia). A sample volume of 8 uL spotted on the paper substrate was found to be sufficient for this study. The ion source was programed to deliver the extraction/spray solvent to the plastic cassette plate at an optimal rate to extract and elute analytes to the tip of the paper for analysis. A solvent volume of 150 uL was found to be optimal for extraction (1 min) and achieving a stable spray throughout the duration of the analysis (1.2 min).

3.2. Method validation

The success of the validation was assessed by evaluating the linearity, limits of detection (LOD), lower limit of quantitation (LLOQ), accuracy (%bias), precision (%CV), carryover, matrix effects, stability, endogenous interference, exogenous interference, and metabolic interference. Fig. 2 represents an overlay of eight calibration curves run over the course of 30 days for remdesivir and its active metabolite, GS-441524. The calibration curves were linear over the concentration range of 20–5000 and 100–25000 ng/mL for remdesivir and GS-441524, respectively. The average coefficients of determination (R^2) for remdesivir and GS-441524 were 0.99 and 1.00, respectively, with an average relative error of the slope of 2% for both analytes (Table 2). The average calculated LODs for remdesivir and its metabolite, GS-441524, were 16 ng/mL and 83 ng/mL, while the average calculated LLOQs were 54 ng/mL and 277 ng/mL, respectively. The measured LLOQs (lowest QC concentrations) for remdesivir and its metabolite, GS-441524, were 80 ng/mL and 400 ng/mL, respectively.

The accuracy and precision of the assay were assessed by analyzing seven plasma-based calibrants and four plasma-based quality control samples ((QC-LLOQ (quality control-lower limit of quantification), QC-low, QC-middle, and QC-high)) on eight different days. The intra-day precision (%CV) and accuracy (%bias) were 1.1–6.4% and within ± 8.5% for remdesivir and 2.4–8.1% and within ± 15% for GS-441524. The inter-day precision (%CV) and accuracy (%bias) were 8.5–11.1% and within ± 10.1% for remdesivir and 7.8–13.8% and within ± 10.8% for GS-441524. Table 3 shows the inter- and intra-day precision (%CV) and accuracy (%bias) data over the eight different runs.

Exogenous interference from Captisol, an additive utilized in remdesivir formulations, and metabolic interference from GS-704227 were evaluated and deemed negligible (*p*-value = >0.05). Additionally, we analyzed endogenous interference from hemolysis, icterus, and lipidemia on remdesivir and GS-441524 QC results. Hemolytic, icteric, and lipidemic samples all passed within the established ± 25% acceptance criteria, with at least 2/3 of samples in each QC level passing within ± 15%, indicating no interference should be seen for these types of samples. To assess relative matrix effects, we prepared and evaluated six different single donor lots of plasma and assessed the variation of the

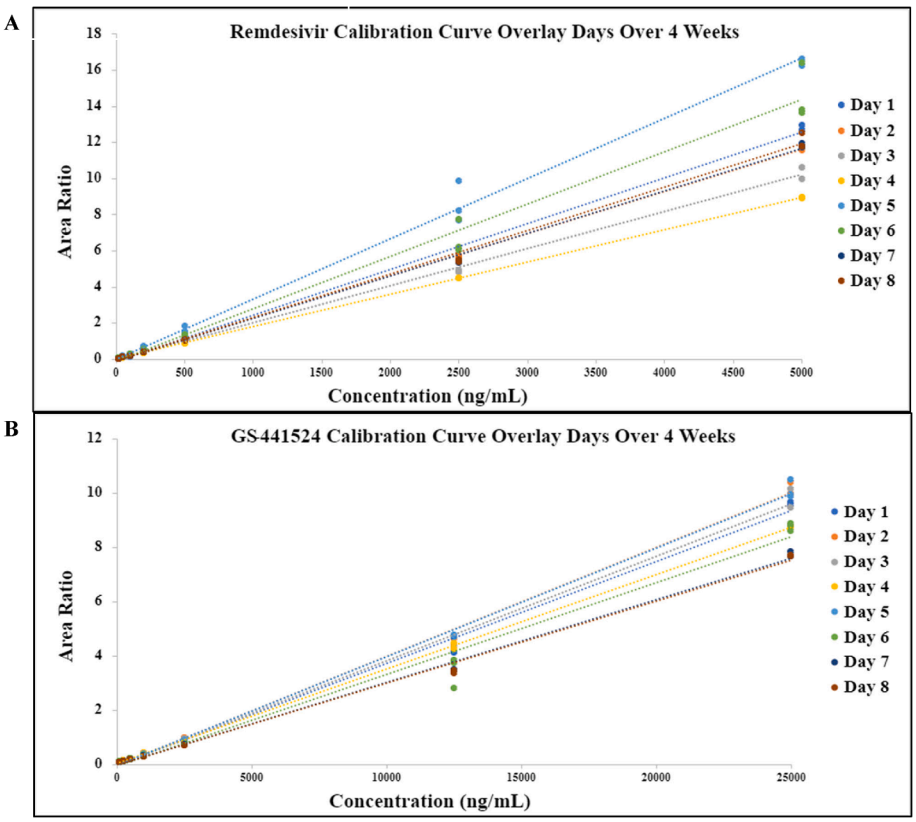

Fig. 2. Calibration curve overlay for remdesivir (A) and its active metabolite GS-441524 (B) over the course of 30 days. Data were collected over eight days (two repeat samples at each level combined to form a single calibration curve per day). Linearity ranged from 0.99 to 1.00.

Table 2
Data were collected over the course of 30 days for eight separate runs. The standard deviation of the calculated LOD is also shown. LOD = 3*(standard error of the intercept/slope). LLOQ = 10*(standard error of the intercept/slope). The measured LLOQ is representative of the QCs with the lowest concentration.

Target	Average R^2	Average Rel. Error of Slope	Average LOD* (ng/mL)	Average LLOQ* (ng/mL)	Measured LLOQ (ng/mL)	EC50 [52–54,57]
Remdesivir	1.00	1.96%	16 ± 7	54	80	398 ng/mL‡ – 16,200 ng/mL¥
GS-441524	1.00	1.76%	83 ± 23	277	400	137 ng/mL¥ –317 ng/mL‡

* Across eight days.
‡ In vitro experiments were conducted in Calu-3 cell lines.
¥ In vitro experiments were conducted in Vero-E6 cell lines.

Table 3
The intra-day accuracy (%bias) and precision (%CV) of the assay. The values show the median of values obtained across eight days. The inter-day accuracy (%bias) and precision (%CV) were calculated for every replicate across eight days. %Bias = (grand mean of calculated concentration-nominal concentration/nominal concentration)*100. %CV = (standard deviation/mean)*100. The QC concentrations were 80 ng/mL (QC LLOQ), 250 ng/mL (QC low), 500 ng/mL (QC medium), 5000 ng/mL (QC high) for remdesivir and 400 ng/mL (QC LLOQ), 1250 ng/mL (QC low), 2500 ng/mL (QC medium), and 25000 ng/mL (QC high) for GS-441524, respectively.

Analyte	QC LLOQ		QC Low		QC Medium		QC High	
	CV (%)	Bias (%)	CV (%)	Bias (%)	CV (%)	Bias (%)	CV (%)	Bias (%)
Intra-day								
Remdesivir	4.2	8.5	6.4	−3.7	3.2	−6.7	1.1	3.0
GS-441524	8.1	5.1	4.7	−15.0	2.6	−5.5	2.4	−4.1
Inter-day								
Remdesivir	11.1	10.1	10.4	−2.2	10.9	−3.7	8.5	4.8
GS-441524	13.8	0.4	12.5	−10.8	7.8	−9.5	8.4	−4.1

calibration slopes (Table 4). The slopes varied by 3% for both remdesivir and GS-441524, which suggests there were no significant matrix effects across different plasma lots. Additionally, no carryover was observed during the validation.

3.3. Stability study

The stability of the stock and spiking solutions were evaluated over the course of four months. No degradation was seen in either set of solutions. The plasma calibrants were stable at −20 °C; however, degradation for the 4 °C and room temperature samples was seen beginning at

Table 4
Average relative error of the slope, LOD, and LOQ for six single donor lots of plasma for remdesivir and GS-441524. LOD = 3*(standard error of the intercept/slope). LLOQ = 10*(standard error of the intercept/slope).

Target	%CV of Slope	Average LOD Across 6 donors (ng/mL)	Average LLOQ Across 6 donors (ng/mL)
Remdesivir	3%	13	43
GS-441524	3%	81	270

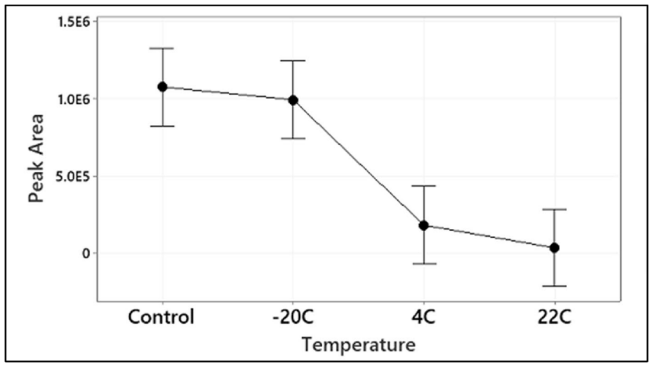

Fig. 3. Interval plot depicting changes in the peak area based on temperature condition for remdesivir on Day 14 of the degradation study. Dots represent mean data for three repeats. Bars represent the 95% confidence interval from the pooled standard deviation.

Day 7. Fig. 3 shows an interval plot for the peak areas with 95% confidence limits for liquid plasma calibrants at the lowest QC level (QC4) staged by temperature condition for remdesivir.

A one-way analysis of variance (ANOVA) was performed on the various QC levels for the different temperature conditions on different days. This test indicated a significantly significant decrease in peak area under the curve (AUC) temperature conditions at day 7 (p-value = 0.000 at alpha = 0.05) for the 4 °C and room temperature (22 °C) samples. A Dunnett's multiple comparison test was also performed to assess which temperature groups differed from the control group (−20 °C). Data indicated that both the 4 °C and room temperature (22 °C) had statistically different peak areas from the control. No degradation was seen for dried plasma spots regardless of temperature or day.

4. Discussion

Reported herein is the development and validation of the first PS-MS/MS method quantitating remdesivir and its active metabolite, GS-441524. The calibration curves for the two analytes showed excellent linearity (average $R^2 = 0.99 – 1.00$) over the course of 30 days evaluated in eight different runs across the measured ranges. An acceptance criteria of ≤ 25% for the accuracy and precision of the nominal concentrations for QCs was chosen before beginning the validation. Broader acceptance criteria was set *a priori,* because this was the first PS-MS/MS anti-viral assay of its kind, a proof-of-concept study, and therapeutic windows for remdesivir and GS-441524 are not yet well-established *in vivo*. Despite the higher acceptance criterion established at the beginning of the validation, overall precision (%CV) and accuracy (%bias) were ≤ 15% and within ± 15%, highlighting the quantitative capabilities of this method. Of the eight batches run, only QC3 and QC4 on one batch day for remdesivir and QC3 on two batch days for GS-441524 did not meet the recommended FDA criteria that 50% of QCs at each concentration level should be ≤ 15% of the nominal concentration (≤ 20% at the QC-LLOQ); however, they did meet our initial acceptance criterion of ≤ 25%. All data were included as it met our initial acceptance criterion; however, our data suggest stricter criteria may be used, and it would be an appropriate adjustment for a cross-validation to further evaluate the fitness of the assay against clinical samples as more information regarding therapeutic windows are established *in vivo*.

Analytical assays can be susceptible to relative matrix effects arising from the use of bio-fluids from different individuals. One method to assess relative matrix effects is by evaluating variability in the slope of the calibration curve in multiple single donor plasma lots [42]. The consistency of the calibration slope among different plasma lots assesses the ability to quantify an analyte in one plasma sample while collecting calibration curves in different lots of plasma. Assessment of matrix effects in this manner has been previously used in a PS-MS/MS assays for citalopram [39] and anti-fungal drugs [33]. The variation in slopes was 3% for remdesivir and GS-441524. This variation arising from matrix was no greater than normal run-to-run variability and on par with relative standard deviation; therefore, the assay was deemed to be free of any relative matrix effects.

In order to avoid under- or over-estimation of the target analytes, endogenous and exogenous interferences were assessed via analysis of drug-free plasma from several donors. Hemolytic, icteric, and lipidemic samples all passed within the established acceptance criteria indicating no interference should be seen for these types of samples. Assessment of one possible exogenous interference from Captisol, which is utilized in remdesivir formulations, did not reveal any interference. Investigation into other possible exogenous interferents, such as drugs commonly utilized in patient treatment, is still needed and is a limitation of this study. Another source of possible interference are labile metabolites of the parent drug that can fragment in-source to yield the same fragment ions as the parent drug. The presence of the remdesivir metabolite, GS-704227, did not reveal interference. Other possible interferents, GS-441524-MP and GS-443902, were not assessed, because they were unavailable at the time of experimentation and manuscript assembly.

The main products of degradation are likely to be the breakdown of the prodrug, remdesivir, by plasma esterases to GS-704277 and conversion of existing or newly-formed GS-704277 to GS-441524 [6]. A temperature and time study was performed to assess stability of remdesivir. A one-way analysis of variance (ANOVA) performed on various QC levels for the temperature conditions on different days showed a statistically significant difference between temperature conditions on Day 7, indicated by a p-value of 0.000. These findings indicated that degradation could occur if samples are improperly stored. It also indicated that the same plasma calibrators could potentially be used for at least a month and still yield accurate quantitative results if stored at −20 °C. Data indicated that dried plasma spots are stable regardless of storage conditions for up to a month, meaning that plasma calibrants for calibration curves could be pre-spotted, dried, and stored for future use. The SRM transitions for GS-441524 were monitored during the experiment, and there was no increase in peak area to suggest that remdesivir significantly degraded into this analyte during our study. While degradation of remdesivir is not a concern at −20 °C in our study, degradation in clinical samples will need to be assessed due to differences in sample collection, storage, and analysis processes. Results from plasma stability studies of remdesivir, GS-704277, and GS-441524 conducted by Xiao, *et al.*, confirmed the need for formic acid as a stabilizing agent upon clinical sample collection to prevent conversion of remdesivir to GS-704277 and conversion of GS-704277 to GS-441524 at room temperature and −4°C [22]. It is recommended that a follow-up study with remnant clinical samples be conducted during cross-validation to further assess for possible overestimation of GS-441524 utilizing our assay.

From a clinical standpoint, the measured lower limits of quantitation (LLOQs) were well below the effective concentration for 50% *in vitro* inhibition of the virus (EC50 [45–47]) for remdesivir making this a suitable method for multi-dose PK/PD modelling studies, TDM and toxicity assessment [12]. However, lack of accurate quantitation at lower ng/mL concentrations may make it inadequate for use in single-dose PK/PD modelling studies. As studies to determine the effective concentration are *in vitro* and tend to differ by virus and cell line, further *in vivo* studies are needed to assess the effect of remdesivir on active

SARS-CoV-2 viral replication, which may not always correlate with *in vitro* studies.

As for the active metabolite, GS-441524, it is unclear how much anti-viral activity it is providing in the setting of SARS-CoV-2 as human PK/PD studies show that the maximum plasma concentration does not exceed ~150–250 ng/mL (dependent on the dosing of remdesivir; current recommended remdesivir dosing is 200 mg on Day 1 followed by 100 mg on Days 2–5) [12]. EC50s reported for GS-441524 are 137 ng/mL to 317 ng/mL (Table 2) [46,48]. Unfortunately, hepatic metabolism of remdesivir results in dose-limiting liver toxicity, which excludes further dose escalation to study any anti-viral effect of GS-441524, *in vivo* [49,50]. In addition, human clinical drug trials have not been conducted exploring the GS-441524 molecule as an anti-viral therapy for SAR-CoV-2 despite promising *in vitro* studies. To date, GS-441524 for use against coronavirus infections has only been studied in animals [48,51]. Overall, GS-441524 appears to be overlooked as it is the most persistent metabolite in plasma, most prominent metabolite in the lung following remdesivir infusion, and less likely to cause liver toxicity [52–55]. It is possible that further exploration of this metabolite as an anti-viral agent will be conducted for coronaviruses, as well as other single-stranded RNA viruses, in the future. Overall, establishing sensitive assays for this molecule will be beneficial as future studies on its efficacy are developed and conducted.

One major benefit of this assay is the use of pre-manufactured cassette plates, an automated PS source with plate-loader magazine unit and bar-code technology, and integrated software for method development, which allowed for the automated analysis of up to 240 samples. However, one limitation with our GS-441524 assay is the higher LOD and LLOQs when compared to known LC-MS/MS methods [18,19,21–23]. The higher LLOQ may limit its use for PK/PD studies; therefore, further steps to improve its sensitivity need to be explored. Whatman grade 31ET chromatography paper is a cellulose-based paper that is easily available, manufacturable, and durable. It is the paper utilized in the pre-manufactured cassettes for the automated Verispray source, and it has been utilized in many PS-MS studies to date. Overall, it shows fairly good performance across many compound groups [56]. In another publication, we explored paper substrate and solvent combinations for a number of different drug classes, including remdesivir and other anti-virals agents [57]. We found that a glass fiber paper with an isopropanol solvent significantly increased the analyte peak AUC and average S/B ratio for remdesivir. While we did not study GS-441524, it is possible similar improvements could be realized for GS-441524 as the glass fiber paper tended to perform well with hydrophilic molecules. We did not use the glass fiber paper in this study, because we preferred to use currently-available pre-manufactured cassettes and automated plug-and-play technology to make the method more easily employable in clinical labs. The glass fiber paper is not commercially available in the pre-manufactured plates and must be prepared, laser-cut in house, and loaded manually into the plates.

5. Conclusion

We report, herein, the first PS-MS/MS assay for the anti-viral agent remdesivir and its active metabolite, GS-441524. The calibration curves for the two antiviral agents showed excellent linearity (average R^2 = 0.99–1.00) across the calibration ranges. The inter- and intra-day precision for both analytes was less than 11.2% and accuracy (%bias) was within ± 15%. Plasma calibrant stability was assessed and degradation were seen beginning at Day 7 for plasma calibrants kept at 4 °C and room temperature. The plasma calibrants were stable at −20 °C during the course of the 21 day stability study. No degradation was seen at any temperature for dried plasma spots during the duration of the stability study. No interference, matrix effects, or carryover was discovered during the validation process. Overall, run time was less than for reported LC-MS/MS methods, and despite the need for 1 h of drying, no sample preparation was required. The utilization of an automated system was another advantage in terms of workflow. Further studies are needed to determine if the assay is comparable to reported LC-MS/MS methods by conducting a cross-validation between LC-MS/MS and PS-MS/MS utilizing clinical specimens. In addition, further studies improving the sensitivity at lower concentrations for the GS-441524 assay are needed, as future studies exploring its viability and efficacy for use as an anti-viral agent will likely be conducted. Overall, the developed PS-MS/MS method is a rapid quantitation tool for remdesivir and its active metabolite, GS-441524 and may prove to be a useful for future clinical research studies.

Declaration of Competing Interest

The authors declare the following financial interests/personal relationships which may be considered as potential competing interests: The authors report financial support from Thermo Scientific for portions of this work. Dr. Manicke is an inventor on the patent “Ion Generation using Wetted Porous Material” issued to Purdue Research Foundation.

Acknowledgements

This work was supported by the National Institutes of Health [T32HD069047] and Thermo Scientific.

References

[1] S. Kung, M. Doppen, M. Black, I. Braithwaite, C. Kearns, M. Weatherall, R. Beasley, N. Kearns, Underestimation of COVID-19 mortality during the pandemic, ERJ Open Res. 7 (1) (2021) 1–7.
[2] M. Piccininni, J.L. Rohmann, L. Foresti, C. Lurani, T. Kurth, Use of all cause mortality to quantify the consequences of covid-19 in Nembro, lombardy: descriptive study, BMJ. 369 (8248) (2020) 1–7.
[3] A. Vieira, V.R. Peixoto, P. Aguiar, A. Abrantes, Rapid estimation of excess mortality during the COVID-19 pandemic in portugal-beyond reported deaths, J. Epidemiol. Glob Health 10 (3) (2020) 209–213.
[4] J.J. Malin, I. Suárez, V. Priesner, G. Fätkenheuer, J. Rybniker, Remdesivir against COVID-19 and other viral diseases, Clin. Microbiol. Rev. 34 (1) (2020) 1–21.
[5] A. Cho, O.L. Saunders, T. Butler, L. Zhang, J. Xu, J.E. Vela, J.Y. Feng, A.S. Ray, C. U. Kim, Synthesis and antiviral activity of a series of 1'-substituted 4-aza-7,9-dideazaadenosine C-nucleosides, Bioorg. Med. Chem. Lett. 22 (8) (2012) 2705–2707.
[6] R.T. Eastman, J.S. Roth, K.R. Brimacombe, A. Simeonov, M. Shen, S. Patnaik, M. D. Hall, Remdesivir: a review of its discovery and development leading to emergency use authorization for treatment of COVID-19, ACS Cent. Sci. 6 (5) (2020) 672–683.
[7] T.K. Warren, R. Jordan, M.K. Lo, A.S. Ray, R.L. Mackman, V. Soloveva, D. Siegel, M. Perron, R. Bannister, H.C. Hui, N. Larson, R. Strickley, J. Wells, K.S. Stuthman, S.A. Van Tongeren, N.L. Garza, G. Donnelly, A.C. Shurtleff, C.J. Retterer, D. Gharaibeh, R. Zamani, T. Kenny, B.P. Eaton, E. Grimes, L.S. Welch, L. Gomba, C. L. Wilhelmsen, D.K. Nichols, J.E. Nuss, E.R. Nagle, J.R. Kugelman, G. Palacios, E. Doerffler, S. Neville, E. Carra, M.O. Clarke, L. Zhang, W. Lew, B. Ross, Q. Wang, K. Chun, L. Wolfe, D. Babusis, Y. Park, K.M. Stray, I. Trancheva, J.Y. Feng, O. Barauskas, Y. Xu, P. Wong, M.R. Braun, M. Flint, L.K. McMullan, S.-S. Chen, R. Fearns, S. Swaminathan, D.L. Mayers, C.F. Spiropoulou, W.A. Lee, S.T. Nichol, T. Cihlar, S. Bavari, Therapeutic efficacy of the small molecule GS-5734 against Ebola virus in rhesus monkeys, Nature. 531 (7594) (2016) 381–385.
[8] J. Grein, N. Ohmagari, D. Shin, G. Diaz, E. Asperges, A. Castagna, T. Feldt, G. Green, M.L. Green, F.-X. Lescure, E. Nicastri, R. Oda, K. Yo, E. Quiros-Roldan, A. Studemeister, J. Redinski, S. Ahmed, J. Bernett, D. Chelliah, D. Chen, S. Chihara, S.H. Cohen, J. Cunningham, A. D'Arminio Monforte, S. Ismail, H. Kato, G. Lapadula, E. L'Her, T. Maeno, S. Majumder, M. Massari, M. Mora-Rillo, Y. Mutoh, D. Nguyen, E. Verweij, A. Zoufaly, A.O. Osinusi, A. DeZure, Y. Zhao, L. Zhong, A. Chokkalingam, E. Elboudwarej, L. Telep, L. Timbs, I. Henne, S. Sellers, H. Cao, S.K. Tan, L. Winterbourne, P. Desai, R. Mera, A. Gaggar, R.P. Myers, D. M. Brainard, R. Childs, T. Flanigan, Compassionate use of remdesivir for patients with severe covid-19, N. Engl. J. Med. 382 (24) (2020) 2327–2336.
[9] J.H. Beigel, K.M. Tomashek, L.E. Dodd, A.K. Mehta, B.S. Zingman, A.C. Kalil, E. Hohmann, H.Y. Chu, A. Luetkemeyer, S. Kline, D. Lopez de Castilla, R. W. Finberg, K. Dierberg, V. Tapson, L. Hsieh, T.F. Patterson, R. Paredes, D. A. Sweeney, W.R. Short, G. Touloumi, D.C. Lye, N. Ohmagari, M.-D. Oh, G.M. Ruiz-Palacios, T. Benfield, G. Fätkenheuer, M.G. Kortepeter, R.L. Atmar, C.B. Creech, J. Lundgren, A.G. Babiker, S. Pett, J.D. Neaton, T.H. Burgess, T. Bonnett, M. Green, M. Makowski, A. Osinusi, S. Nayak, H.C. Lane, Remdesivir for the treatment of Covid-19 — final report, N. Engl. J. Med. 383 (19) (2020) 1813–1826.
[10] Y. Wang, D. Zhang, G. Du, R. Du, J. Zhao, Y. Jin, S. Fu, L. Gao, Z. Cheng, Q. Lu, Y. Hu, G. Luo, K. Wang, Y. Lu, H. Li, S. Wang, S. Ruan, C. Yang, C. Mei, Y. Wang, D. Ding, F. Wu, X. Tang, X. Ye, Y. Ye, B. Liu, J. Yang, W. Yin, A. Wang, G. Fan, F. Zhou, Z. Liu, X. Gu, J. Xu, L. Shang, Y. Zhang, L. Cao, T. Guo, Y. Wan, H. Qin,

Y. Jiang, T. Jaki, F.G. Hayden, P.W. Horby, B. Cao, C. Wang, Remdesivir in adults with severe COVID-19: a randomised, double-blind, placebo-controlled, multicentre trial, Lancet. 395 (10236) (2020) 1569–1578.
[11] C.D. Spinner, R.L. Gottlieb, G.J. Criner, J.R. Arribas López, A.M. Cattelan, A. Soriano Viladomiu, O. Ogbuagu, P. Malhotra, K.M. Mullane, A. Castagna, L.Y. A. Chai, M. Roestenberg, O.T.Y. Tsang, E. Bernasconi, P. Le Turnier, S.C. Chang, D. SenGupta, R.H. Hyland, A.O. Osinusi, H. Cao, C. Blair, H. Wang, A. Gaggar, D. M. Brainard, M.J. McPhail, S. Bhagani, M.Y. Ahn, A.J. Sanyal, G. Huhn, F. M. Marty, Effect of remdesivir vs standard care on clinical status at 11 days in patients with moderate COVID-19: a randomized clinical trial, JAMA. 324 (11) (2020) 1048–1057.
[12] R. Humeniuk, A. Mathias, H. Cao, A. Osinusi, G. Shen, E. Chng, J. Ling, A. Vu, P. German, Safety, tolerability, and pharmacokinetics of remdesivir, an antiviral for treatment of COVID-19 Healthy Subjects, Clin. Transl. Sci. 13 (5) (2020) 896–906.
[13] N. Venisse, G. Peytavin, S. Bouchet, M.-C. Gagnieu, R. Garraffo, R. Guilhaumou, C. Solas, ANRS-AC43 Clinical Pharmacology Committee, SFPT Therapeutic Drug Monitoring and Treatment Personalization group, Concerns about pharmacokinetic (PK) and pharmacokinetic-pharmacodynamic (PK-PD) studies in the new therapeutic area of COVID-19 infection, Antiviral Res. 181 (104866) (2020) 1–9.
[14] J. Charan, R.J. Kaur, P. Bhardwaj, M. Haque, P. Sharma, S. Misra, B. Godman, Rapid review of suspected adverse drug events due to remdesivir in the WHO database; findings and implications, Expert Rev. Clin. Pharmacol. 14 (1) (2021) 95–103.
[15] Y. Shen, W. Eades, B. Yan, The COVID-19 medicine remdesivir is therapeutically activated by carboxylesterase-1, and excessive hydrolysis increases cytotoxicity, Hepatol. Commun. 5 (9) (2021) 1622–1623.
[16] W. Zhu, L. Song, H. Zhang, L. Matoney, E. LeCluyse, B. Yan, Dexamethasone differentially regulates expression of carboxylesterase genes in humans and rats, Drug Metab. Dispos. 28 (2) (2000) 186–191.
[17] Y. Shen, W. Eades, B. Yan, Remdesivir potently inhibits carboxylesterase-2 through covalent modifications: signifying strong drug-drug interactions, Fundam. Clin. Pharmacol. 35 (2) (2021) 432–434.
[18] K. Habler, M. Brügel, D. Teupser, U. Liebchen, C. Scharf, U. Schönermarck, M. Vogeser, M. Paal, Simultaneous quantification of seven repurposed COVID-19 drugs remdesivir (plus metabolite GS-441524), chloroquine, hydroxychloroquine, lopinavir, ritonavir, favipiravir and azithromycin by a two-dimensional isotope dilution LC-MS/MS method in human serum, J. Pharm. Biomed. Anal. 196 (113935) (2021) 1–8.
[19] R. Nguyen, J.C. Goodell, P.S. Shankarappa, S. Zimmerman, T. Yin, C.J. Peer, W. D. Figg, Development and validation of a simple, selective, and sensitive LC-MS/MS assay for the quantification of remdesivir in human plasma, J. Chromatogr. B. 1171 (12264) (2021) 1–7.
[20] R.R. Pasupuleti, P.-C. Tsai, V.K. Ponnusamy, A. Pugazhendhi, Rapid determination of remdesivir (SARS-CoV-2 drug) in human plasma for therapeutic drug monitoring in COVID-19-Patients, Process Biochem. 102 (2021) 150–156.
[21] A. Reckers, A.H.B. Wu, C.M. Ong, M. Gandhi, J. Metcalfe, R. Gerona, A combined assay for quantifying remdesivir and its metabolite, along with dexamethasone, in serum, J. Antimicrob. Chemother. 76 (7) (2021) 1865–1873.
[22] D. Xiao, K.H. John Ling, T. Tarnowski, R. Humeniuk, P. German, A. Mathias, J. Chu, Y.S. Chen, E. van Ingen, Validation of LC-MS/MS methods for determination of remdesivir and its metabolites GS-441524 and GS-704277 in acidified human plasma and their application in COVID-19 related clinical studies, Anal. Biochem. 617 (114118) (2021) 1–12.
[23] J.C. Alvarez, P. Moine, I. Etting, D. Annane, I.A. Larabi, Quantification of plasma remdesivir and its metabolite GS-441524 using liquid chromatography coupled to tandem mass spectrometry. Application to a Covid-19 treated patient, Clinl. Chem. Lab. Med. 58 (9) (2020) 1461–1468.
[24] P.J. Jannetto, R.L. Fitzgerald, Effective use of mass spectrometry in the clinical laboratory, Clin. Chem. 62 (1) (2016) 92–98.
[25] W. Clarke, J.M. Rhea, R. Molinaro, Challenges in implementing clinical liquid chromatography–tandem mass spectrometry methods – seeing the light at the end of the tunnel, J. Mass Spectrom. 48 (7) (2013) 755–767.
[26] H. Wang, J. Liu, R.G. Cooks, Z. Ouyang, Paper spray for direct analysis of complex mixtures using mass spectrometry, Angew. Chem. Int. Ed. 49 (5) (2010) 877–880.
[27] J. Liu, H. Wang, N.E. Manicke, J.M. Lin, R.G. Cooks, Z. Ouyang, Development, characterization, and application of paper spray ionization, Anal. Chem. 82 (6) (2010) 2463–2471.
[28] Q. Yang, H. Wang, J.D. Maas, W.J. Chappell, N.E. Manicke, R.G. Cooks, Z. Ouyang, Paper spray ionization devices for direct, biomedical analysis using mass spectrometry, Int. J. Mass Spectrom. 312 (2012) 201–207.
[29] R.D. Espy, A.R. Muliadi, Z. Ouyang, R.G. Cooks, Spray mechanism in paper spray ionization, Int. J. Mass Spectrom. 325–327 (2012) 167–171.
[30] R.Z. Shi, E.T.M.E. Gierari, N.E. Manicke, J.D. Faix, Rapid measurement of tacrolimus in whole blood by paper spray-tandem mass spectrometry (PS-MS/MS), Clin Chim Acta. 441 (1) (2015) 99–104.
[31] R.-Z. Shi, E.T.M. El Gierari, J.D. Faix, N.E. Manicke, Rapid measurement of cyclosporine and sirolimus in whole blood by paper spray-tandem mass spectrometry, Clin. Chem. 62 (1) (2016) 295–297.
[32] C. Skaggs, L. Kirkpatrick, W.R.A. Wichert, N. Skaggs, N.E. Manicke, A statistical approach to optimizing paper spray mass spectrometry parameters, Rapid Commun. Mass Spectrom. 34 (7) (2020) 1–7.
[33] C.L. Skaggs, G.J. Ren, E.T.M. Elgierari, L.R. Sturmer, R.Z. Shi, N.E. Manicke, L. M. Kirkpatrick, Simultaneous quantitation of five triazole anti-fungal agents by paper spray-mass spectrometry, Clin. Chem. Lab. Med. 58 (5) (2020) 836–846.
[34] S. D'Aronco, E. Calandra, S. Crotti, G. Toffoli, E. Marangon, B. Posocco, P. Traldi, M. Agostini, Field-assisted paper spray mass spectrometry for the quantitative evaluation of imatinib levels in plasma, Eur. J. Mass Spectrom. 22 (5) (2016) 217–228.
[35] J. Zhao, C. Sharat, P.A. Mehta, K. Mizuno, A.A. Vinks, K.D.R. Setchell, Paperspray ionization mass spectrometry as a tool for predicting real-time optimized dosing of the chemotherapeutic drug melphalan, J. Appl. Lab. Med. 6 (3) (2021) 625–636.
[36] Y. Liu, X.H. Zhang, W.D. Mi, Y.L. Zhou, C.S. Zhang, X.X. Zhang, Rapid determination and continuous monitoring of propofol in microliter whole blood sample during anesthesia by paper spray ionization-mass spectrometry, Anal. Bioanal. Chem. 413 (1) (2021) 279–287.
[37] Y. Su, H. Wang, J. Liu, P. Wei, R.G. Cooks, Z. Ouyang, Quantitative paper spray mass spectrometry analysis of drugs of abuse, Analyst. 138 (16) (2013) 4443–4447.
[38] G.W. Vandergrift, C.G. Gill, Paper spray mass spectrometry: A new drug checking tool for harm reduction in the opioid overdose crisis, J. Mass Spectrom. 54 (9) (2019) 729–737.
[39] N.E. Manicke, P. Abu-Rabie, N. Spooner, Z. Ouyang, R.G. Cooks, Quantitative analysis of therapeutic drugs in dried blood spot samples by paper spray mass spectrometry: an avenue to therapeutic drug monitoring, J. Am. Soc. Mass Spectrom. 22 (9) (2011) 1501–1507.
[40] R.D. Espy, N.E. Manicke, Z. Ouyang, R.G. Cooks, Rapid analysis of whole blood by paper spray mass spectrometry for point-of-care therapeutic drug monitoring, Analyst. 137 (10) (2012) 2344–2349.
[41] FDA, Bioanalytical method validation guidance for industry, in: Food and Drug Administration, White Oaks, Maryland, USA, 2018, pp. 1–44.
[42] B.K. Matuszewski, Standard line slopes as a measure of a relative matrix effect in quantitative HPLC-MS bioanalysis, J. Chromatogr. B 830 (2) (2006) 293–300.
[43] M. Meng, S. Carter, P. Bennet, LC-MS bioanalysis of drugs in hemolyzed and lipemic samples, in: W. Li, J. Zhang, F. Tse (Eds.), Handbook of LC-MS bioanalysis: best practices, experimental protocols, and regulations, John Wiley & Sons, Inc, Hoboken, New Jersey, 2013, pp. 369–379.
[44] A.M. Almeida, M.M. Castel-Branco, A.C. Falcão, Linear regression for calibration lines revisited: weighting schemes for bioanalytical methods, J. Chromatogr. B 774 (2) (2002) 215–222.
[45] A. Frediansyah, F. Nainu, K. Dhama, M. Mudatsir, H. Harapan, Remdesivir and its antiviral activity against COVID-19: a systematic review, Clin. Epidemiol. Glob. Health. 9 (2021) 123–127.
[46] A.J. Pruijssers, A.S. George, A. Schäfer, S.R. Leist, L.E. Gralinksi, K.H. Dinnon, B. L. Yount, M.L. Agostini, L.J. Stevens, J.D. Chappell, X. Lu, T.M. Hughes, K. Gully, D.R. Martinez, A.J. Brown, R.L. Graham, J.K. Perry, V. Du Pont, J. Pitts, B. Ma, D. Babusis, E. Murakami, J.Y. Feng, J.P. Bilello, D.P. Porter, T. Cihlar, R.S. Baric, M.R. Denison, T.P. Sheahan, Remdesivir inhibits SARS-CoV-2 in human lung cells and chimeric SARS-CoV expressing the SARS-CoV-2 RNA polymerase in mice, Cell Rep. 32 (3) (2020) 1–10.
[47] M. Wang, R. Cao, L. Zhang, X. Yang, J. Liu, M. Xu, Z. Shi, Z. Hu, W. Zhong, G. Xiao, Remdesivir and chloroquine effectively inhibit the recently emerged novel coronavirus (2019-nCoV) in vitro, Cell Res. 30 (3) (2020) 269–271.
[48] Y. Li, L. Cao, G. Li, F. Cong, Y. Li, J. Sun, Y. Luo, G. Chen, G. Li, P. Wang, F. Xing, Y. Ji, J. Zhao, Y. Zhang, D. Guo, X. Zhang, Remdesivir metabolite GS-441524 effectively inhibits SARS-CoV-2 infection in mouse models, J. Med. Chem. 65 (4) (2021) 2785–2793.
[49] A. Aleem, G. Mahadevaiah, N. Shariff, J.P. Kothadia, Hepatic manifestations of COVID-19 and effect of remdesivir on liver function in patients with COVID-19 illness, Proc. (Bayl. Univ. Med. Cent.) 34 (4) (2021) 473–477.
[50] R. Zampino, F. Mele, L.L. Florio, L. Bertolino, R. Andini, M. Galdo, R. De Rosa, A. Corcione, E. Durante-Mangoni, Liver injury in remdesivir-treated COVID-19 patients, Hepatol. Int. 14 (5) (2020) 881–883.
[51] V.C. Yan, C.D. Pham, M.J. Yan, A.J. Yan, S. Khadka, K. Arthur, J.J. Ackroyd, D. K. Georgiou, L.E. Roon, L.R. Bushman, P.L. Anderson, C. Li, F.L. Muller, Pharmacokinetics of Orally Administered GS-441524 in Dogs, bioRxiv preprint (2021) 1–18.
[52] M. Tempestilli, P. Caputi, V. Avataneo, S. Notari, O. Forini, L. Scorzolini, L. Marchioni, T. Ascoli Bartoli, C. Castilletti, E. Lalle, M.R. Capobianchi, E. Nicastri, A. D'Avolio, G. D'Avolio, C. Agrati, C.I.S. Group, Pharmacokinetics of remdesivir and GS-441524 in two critically ill patients who recovered from COVID-19, J. Antimicrob Chemother. 75 (10) (2020) 2977–2980.
[53] T.P. Sheahan, A.C. Sims, R.L. Graham, V.D. Menachery, L.E. Gralinski, J.B. Case, S. R. Leist, K. Pyrc, J.Y. Feng, I. Trantcheva, R. Bannister, Y. Park, D. Babusis, M. O. Clarke, R.L. Mackman, J.E. Spahn, C.A. Palmiotti, D. Siegel, A.S. Ray, T. Cihlar, R. Jordan, M.R. Denison, R.S. Baric, Broad-spectrum antiviral GS-5734 inhibits both epidemic and zoonotic coronaviruses, Sci. Transl. Med. 9 (396) (2017) 1–20.
[54] B.N. Williamson, F. Feldmann, B. Schwarz, K. Meade-White, D.P. Porter, J. Schulz, N. van Doremalen, I. Leighton, C.K. Yinda, L. Pérez-Pérez, A. Okumura, J. Lovaglio, P.W. Hanley, G. Saturday, C.M. Bosio, S. Anzick, K. Barbian, T. Cihlar, C. Martens, D.P. Scott, V.J. Munster, E. de Wit, Clinical benefit of remdesivir in rhesus macaques infected with SARS-CoV-2, Nature. 585 (7824) (2020) 273–276.
[55] V.C. Yan, F.L. Muller, Advantages of the parent nucleoside GS-441524 over remdesivir for covid-19 treatment, ACS Med. Chem. Lett. 11 (7) (2020) 1361–1366.
[56] E.M. McBride, P.M. Mach, E.S. Dhummakupt, S. Dowling, D.O. Carmany, P. S. Demond, G. Rizzo, N.E. Manicke, T. Glaros, Paper spray ionization: applications and perspectives, TrAC Trends Analyt. Chem. 118 (2019) 722–730.
[57] C. Skaggs, L. Kirkpatrick, C. Nguyen, S. Dowling, H. Zimmerman, G. Ren, N. Manicke, Simultaneous optimization of paper spray substrates and solvents for hydrophilic and hydrophobic molecules, Int. J. Mass Spectrom. 470 (116705) (2021) 1–20.